BAU Journal - Science and Technology

Volume 3 | Issue 1
ISSN: 2706-784X

Article 3

December 2021

INVESTIGATION OF THE EXPERIMENTAL AND NUMERICAL FLEXURAL BEHAVIOR OF INNOVATIVE TOTALLY ENCASED COMPOSITE BEAMS

Nour Wehbi
Lecturer, Faculty of Engineering, Beirut Arab University, Lebanon, n.wehbi@bau.edu.lb

Adnan Masri
Professor, Faculty of Engineering, Beirut Arab University, Beirut, Lebanon, amasri@bau.edu.lb

Oussama Baalbaki
Professor, Faculty of Engineering, Beirut Arab University, Beirut, Lebanon, obaalbaki@bau.edu.lb

INVESTIGATION OF THE EXPERIMENTAL AND NUMERICAL FLEXURAL BEHAVIOR OF INNOVATIVE TOTALLY ENCASED COMPOSITE BEAMS

Abstract

Composite steel-concrete beams have been widely used in long span construction and high rise buildings due to their favorable behavior in terms of high strength, stiffness, and ductility. In this research, the flexural behavior of an innovative steel-concrete composite section is investigated experimentally and verified numerically using ABAQUS software. The studied section is composed of steel tubular specimen or steel hollow pipe totally encased in concrete in the absence of any flexural or shear reinforcement. Instead, steel mesh wraps are used around the tubular steel specimen to provide sufficient steel-concrete bond. All of the studied beams have the same 3m length and T-section dimensions to provide adequate comparison of results. The influence of using different percentages of steel mesh wraps around the steel specimen and the structural steel shape effect on the failure mode and ultimate flexural capacity were investigated. It was found that the ABAQUS model has provided excellent simulation of the flexural response of the studied beams with acceptable difference in results as compared to those obtained from experimental testing. Besides, the presence of steel mesh wraps at highly compressive damaged locations have prevented concrete spalling and crushing in these zones by ensuring sufficient steel-concrete bond.

Keywords

ABAQUS Model, composite beams, total encasement, experimental investigation, flexural behavior

1. INTRODUCTION

The usage of composite steel- concrete structures has been enormously used in long -span bridges, high rise buildings, stadiums, and offshore structures [1-5]. Due to the huge research interest in the domain of composite structures, the forms of composite sections are evolving and innovative sections are designed and constructed over the world. This increased demand on composite structures requires the designers to have sound understanding of the behavior and latest design principles of these structures.

One of these enormously used composite sections forms is the concrete filled steel tubes (CFST) that are gaining popularity in bridges and high rise buildings especially under dynamic analysis as highlighted by many authors including Fujikura, S., Fan, H , and Fu,Z. Numerous researches were lunched to better understand the performance of such section type under the influence of several parameters. For instant, Farhan, K. and Shallal, M. aimed to highlight the flexural performance of concrete filled steel tubular beams taking into account several beam lengths and changing the steel section shape between square and circular. The later results showed higher ultimate capacity with favorable performance for circular composite beams over square composite beams. Also, Adithya, T. and Monica Madhuri, N. were interested in studying the bonding mechanism between the internal surface of the steel tube and the concrete by adding Sand coated surface or steel connectors. The results revealed that the difference in bonding mechanism had no significant effect on the flexural performance of the beams. Other parameters of huge interest are related to the effect of tubular steel section thickness and compressive strength on composite beam ultimate capacity and ductility as they were investigated by Usach, C., Figueirido, D., and Piquer, A.

Besides, concrete encased steel sections are increasingly used in buildings accounting for favorable ductility and tensile strength afforded by steel, as well as, stiffness and fire resistance of concrete. As a result, several studies are being lunched to investigate the fire resistance rate of different shapes of concrete- encased steel composite members under several conditions. Some of these studies include concrete-encased CFST columns that was studied by Zhou, K. and built-up steel section completely encased in concrete that was investigated by Wehbi, N. In addition, the flexural behavior studies have shown that concrete encased steel tubular sections (CEST) can provide 40 to 70% improvement in ultimate flexural strength (directly proportional to tube depth), enhanced ductility, and increased elastic deformations compared to reinforced concrete beam of same and 20% higher depth as it was obtained by El Basha, M and his co-authors. Further research was done by Weng, C.C on CEST sections to account for splitting shear failure and recommending the usage of shear connectors when the ratio of the steel flange width to that of concrete width is greater than 0.67. Another important research was launched by Tuma, N. and Aziz, M. to study the influence of the flexural steel reinforcement, usage of shear studs, and location of steel tubular section on the entire flexural performance of CEST specimens. The obtained results showed that the stiffness enhanced obviously by increasing the flexural steel ratio and composite beams with shear studs provide considerable increase in the ultimate capacity over non composite specimens. Also, Neelima, K. and Shingade, V.S explored the effect of shear reinforcement, in composite beams, on their flexural and shear behavior. It was obtained that concrete crushing in diagonal tension occurred in beams lacking shear reinforcement.

In conclusion, the complicated behavior of steel-concrete composite members, having wide range of shapes, is still considered as a source of attraction for researchers aiming to better understand the interaction between the two materials that control the overall performance. The aim of this paper is to evaluate the flexural performance of an innovative T-shape CEST section consisting of hollow rectangular and circular steel sections totally encased in concrete using both ABAQUS numerical analysis as well as experimental testing. The significance of the studied section is being attached to reinforced concrete deck to form a rib in the absence of any shear or flexural reinforcement in the web and any type of shear connectors. Instead, an innovative method of interaction between steel and concrete was created by using wrapped steel mesh allowing the studied section to act as a part of

easily precast long-span floor system. Results of different specimens' ultimate capacities, deflection, and failure modes are displayed and analyzed in the light of several percentages of steel mesh wrapping and different tubular section shapes.

2. EXPERIMENTAL PROGRAM

2.1.Test Specimens

The experimental program consisted of a set of five composite beams of same 3m length, T-section dimensions, and reinforced concrete slab rebars to be tested under flexural loading till failure. This set comprises two groups: The first specimen group is made up from steel tube denoted by ST235 JRH and having dimensions of 160x80x4mm and steel area of 1856mm2. In this group, the studied parameters are related to the percentage of steel tube length being mesh-wrapped in the absence of any reinforcing bars and stirrups as shown in Fig.1.

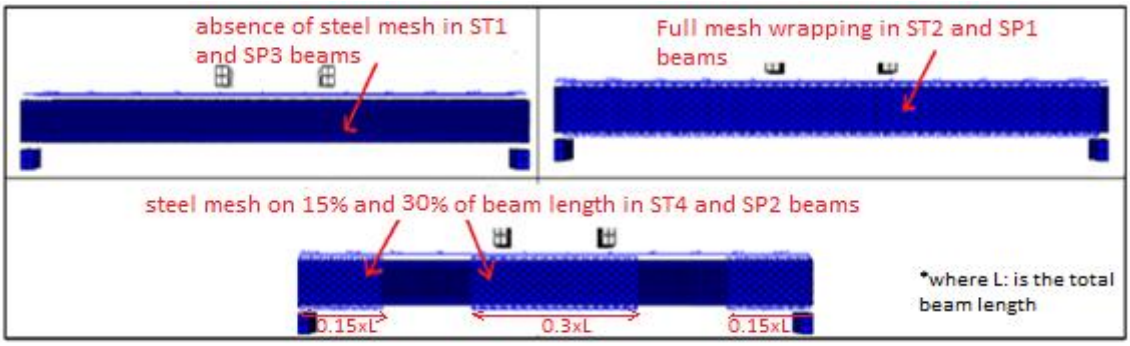

Fig.1: Different Percentages of Steel Mesh Wrapping around Steel Tubular Specimens

The second group was an extension to the research done by [19] aiming to study the influence of steel section shape on the flexural behavior and capacity of the composite section. Therefore, a steel pipe having the same cross section area and location of the center of gravity as that of the steel tube was studied under the same parameters mentioned previously for comparison.

Table1 summarizes the test plan followed in the experimental program to display the studied parameters and Fig.2 provides a schematic representation of the various sections studied. As it can be shown from Table 1, all the specimens were studied under both experimental and numerical investigations except for ST3 and SP3 beams because the numerical model showed loss of composite action and complete spalling at the edges of the beams at ultimate capacity. So, the simulated behavior of ST3 and SP3 specimens was not of interest anymore.

Table 1: Test Plan

Test Group	Specimen	Steel Section (mm)	Mesh (% of beam Length)	Type of study
Group 1	ST.1	ST. 160x80x4	0%	Numerical & experimental
	ST.2	ST. 160x80x4	100%	Numerical & experimental
	ST.3	ST. 160x80x4	30%	Numerical only
	ST.4	ST. 160x80x4	60%	Numerical & experimental
Group 2	SP.1	SP. 127x5	100%	Numerical & experimental
	SP.2	SP. 127x5	60%	Numerical & experimental
	SP.3	SP. 127x5	0%	Numerical only

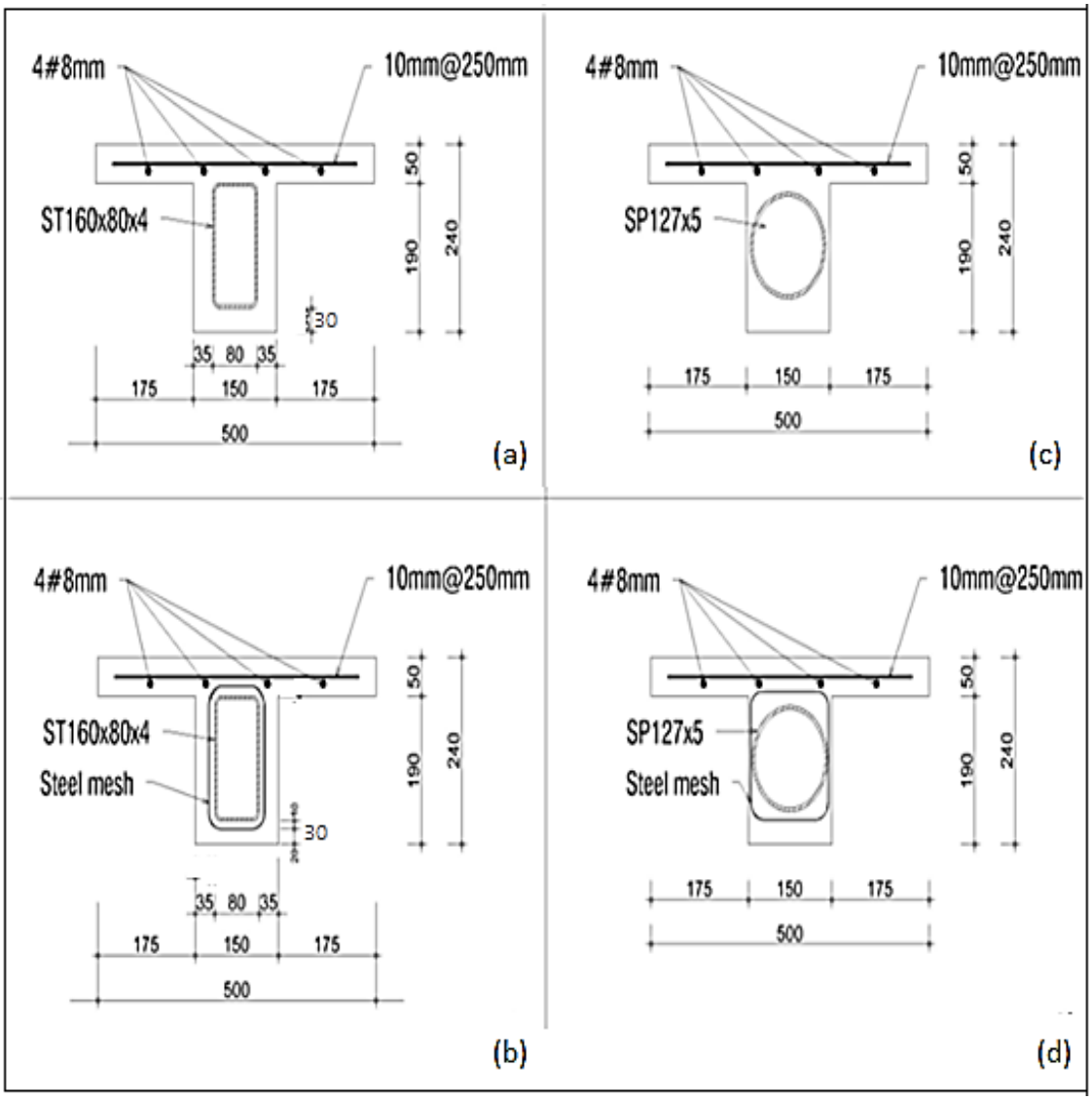

Fig. 2: Studied Composite Sections (dimensions in mm).

2.2 Material Properties

The concrete used in this study has an average compressive strength at 28 days of 24.2 Mpa with mix proportions shown in Table 2. In fact, Polypropylene fiber of 6 mm length was used to limit the cracking and concrete spalling due to the absence of steel reinforcement. Also, the use of small size aggregates was to provide homogeneous mix and avoid segregation resulting from clogging caused by aggregates due to the limited concrete cover thickness.

Whereas the structural steel is of mild steel type denoted by S235JRH having a yielding and ultimate strengths of 280Mpa and 453 Mpa respectively.

Table 2: Concrete Mix Proportions [19]

Material	Corrected batch weight
Cement (Kg/m3)	350
Water (l/m3)	180.8
9.5 mm aggregate	908
Natural sand (Kg/m3)	887
Sikament admixture (Kg/m3)	5.25
Fiber (Kg/m3)	2.1

2.3 Test Setup

The aim of the experimental phase was to investigate the flexural behavior of the composite specimens under the influence of two-point bending loads. During the experimental program, the deflection records provided by linear variable differential transducers (Lvdt) and the corresponding applied loads are registered and monitored through a data acquisition system to allow plotting of the load deflection curves. Fig.3 illustrates a schematic representation for the test setup used.

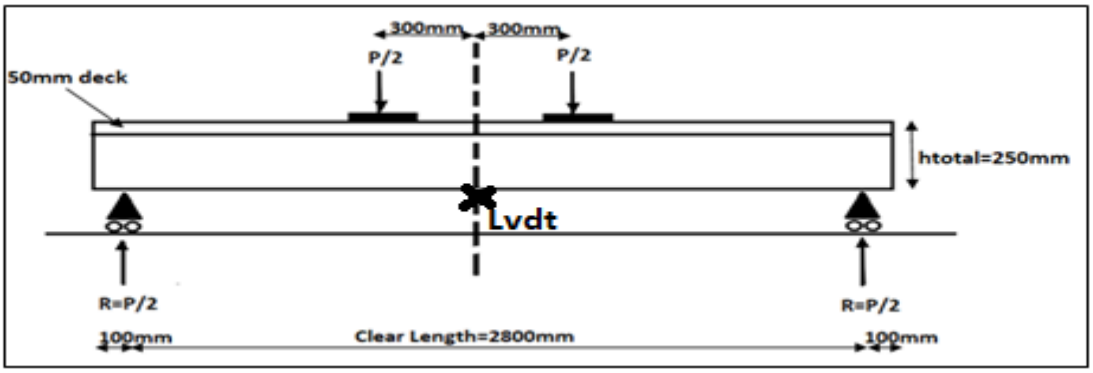

Fig. 3: Test Setup

3. FINITE ELEMENT MODELING

In order to have a guideline for structural engineers to have an accurate prediction of the behavior of composite beams under study, FEM was generated using ABAQUS software for all the seven beams mentioned in the test plan. ABAQUS software has been proven, by several researchers over years, to be an advanced simulation tool that can cover both Standard/Static as well as Dynamic/Explicit phenomena. The mechanical behavior in ABAQUS is defined by Eq. 1 for dynamic state and the simplified Eq. 2 for static analysis.

$$Fs = KU + C\hat{U} + M\ddot{U} \quad (1)$$

$$Fs = KU \quad (2)$$

Where, Fs is the applied force, K is the material stiffness, C is the damping coefficient, M is the mass constant tensor, U is the displacement, Û is the speed generated, and Ü is the acceleration.

In this research, nonlinear standard static analysis was adopted to simulate the behavior of composite beams studied under the influence of incremental load applied till failure. The methodology of material properties definition and assembly generation follow the requirements provided in ABAQUS Manual and will be discussed in the following sections.

3.1 Concrete Damage Plasticity Model (CDP)

The adopted model represents the behavior of concrete material is the continuum plasticity-based damage model denoted by CDP. The CDP model is a built-in model in ABAQUS that assumes two main failure mechanisms of concrete: the tensile cracking and compressive crushing of the material.

In the CDP model, the degradation of elastic stiffness in tension and compression, during the failure mechanisms, are defined by mean of two damage variables: dt and dc. The damage variables can range from a value 0 representing no damage to 1 showing full material damage.

When defining compressive or tensile behavior, tabulated data of the stress versus cracking strain Ɛtck (for tensile behavior) and crushing strain ƐcIn (for compressive behavior) is needed. Where each of the previous strain values is equal to the total strain minus the elastic strain. After that, ABAQUS will automatically convert the cracking and crushing strains to plastic strains according to Eq. 3 and Eq.4.

$$\hat{\varepsilon}_t^{\,pl} = \varepsilon_t^{ck} - \frac{dt}{1-dt} \cdot \frac{\sigma t}{Eo} \tag{3}$$

$$\hat{\varepsilon}_c^{\,pl} = \varepsilon_c^{In} - \frac{dc}{1-dc} \cdot \frac{\sigma c}{Eo} \tag{4}$$

Where Eo is the initial modulus of elasticity of concrete material.

Also, In the CDP model, ABAQUS [20] uses the yield function of Lublineret.al. [21-22] with the modifications developed by Lee and Fenves [23] to account for different evolution of strength under tension and compression. Lubliner's yield function built-in CDP model is defined in Eq. 5 and its parameters are calculated according to Eqs. 6 to Eqn.8.

$$F=\frac{1}{1-\alpha}\left(\bar{q} - 3\alpha\bar{p} + \beta\varepsilon^{pl}\left(\hat{\bar{\sigma}}_{max}\right) - \gamma\left(-\hat{\bar{\sigma}}_{max}\right)\right) - \bar{\sigma_c}\left(\hat{\varepsilon_c}^{\,pl}\right) \geq 0 \tag{5}$$

$$\alpha=\frac{\left(\sigma_{b0}/\sigma_{c0}\right)-1}{2\left(\sigma_{b0}/\sigma_{c0}\right)-1}; 0 \leq \alpha \leq 0.5 \tag{6}$$

$$\beta=\frac{\bar{\sigma}_c\left(\hat{\varepsilon}_c^{\,pl}\right)}{\bar{\sigma}_t\left(\hat{\varepsilon}_t^{\,pl}\right)} * (1-\alpha) - (1+\alpha) \tag{7}$$

$$\gamma=\frac{3(1-K_c)}{2K_c-1} \tag{8}$$

Where, $\bar{\sigma}_{\hat{}\,max}$ is the maximum principle effective stress, σ_{b0}/σ_{c0} is the ratio of constant biaxial compressive yield stress to uniaxial compressive yield stress, Kc is the ratio of the second stress invariant on the tensile meridian to that on the compressive meridian where $0.5 < Kc < 1.0$ having a default value of 0.67, $\bar{\sigma}_c\left(\hat{\varepsilon}_c^{\,pl}\right)$ is the effective compressive cohesions stress, and $\bar{\sigma}_t\left(\hat{\varepsilon}_c^{\,pl}\right)$ is the effective tensile cohesive stress.

3.2 Steel Model: Strain Hardening Plastic Model

The elastic behavior of steel material was modeled by defining elastic behavior of given modulus of elasticity and density. Besides, a non-linear behavior was defined by choosing Plastic material behavior in which the introduced stresses are reversible for the case of tension and compression but the plastic strains generated are irreversible. The stress- inelastic strain data of structural and reinforced steel were taken based on coupon tests done at Beirut Arab University Laboratory.

3.3 Element Definition and Material Interaction

In this research, concrete and structural steel (tube or pipe) are defined as C3D8R (Fig. 4). This material stands for three dimensional, continuum, eight nodded elements with reduced integration. The advantage of the reduced integration is to have only one integration point for each surface of the element and therefore reducing the amount of CPU time needed for analysis. However, the longitudinal rebars, transversal rebars, and stirrups of the control beam, as well as, the reinforced concrete deck reinforcement were generated as T3D2 which represents a two nodded truss (wire) element that takes axial forces.

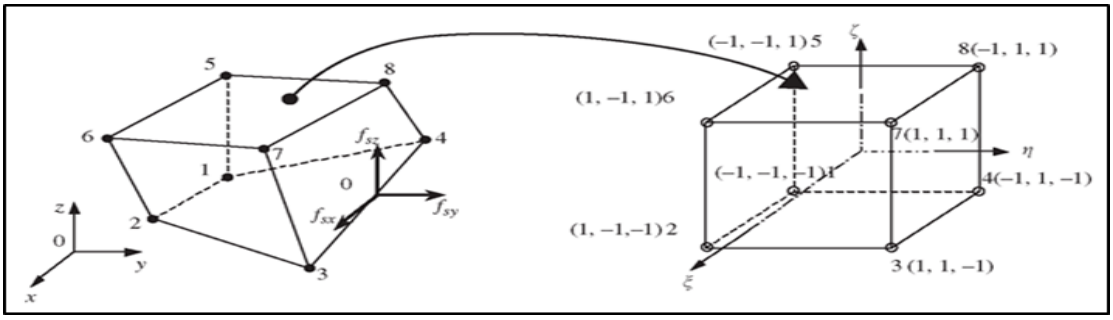

Fig.4: Three-Dimensional Eight Nodded Elements C3D8R

To provide an assembly of different structural parts that act together in a realistic manner, material interaction was defined. The steel reinforcement and steel mesh were defined as embedded elements in the host member (concrete) to ensure full bond and strain compatibility between the two materials. However, the interaction between the structural steel (tube or pipe) and concrete was defined as a surface contact providing it with normal and tangential properties to ensure sufficient load transfer and friction between the two materials.

4. RESULTS: VALIDATION OF FEM

The numerical phase of this research started by comparing the results obtained from the experimental testing to those generated by the defined FEM using ABAQUS software to ensure the reliability of the model generated. The results of interest are related to the load-deflection records and failure modes of the composite specimens. The specimens that are considered in this section are those which have been tested experimentally including: ST1, ST2, ST4, SP1, and SP3.

4.1 ST1 Specimen:

As it can be noticed from Fig. 5, ABAQUS software provided excellent simulation of the real flexural behavior of ST1 beam showing very close results regarding the load-deflection records. Besides, the difference of ultimate capacity and deflection, between numerical and experimental results, was 6.2% and 5.9% respectively.

Also, Fig.6 shows the validation of numerical results of ST1 in terms of the failure mode. For instant, the formation of wide horizontal concrete tensile damage near the supports of the studied beam (Fig.6(b)) has led to the formation of high compression damage above 83% (Fig. 6(c)) which can be explained by concrete total crushing satisfying the real experimental case (Fig. 6(a)). However, at the mid span only wide tensile cracks, without spalling, were recorded as the compression damage was low at that instant.

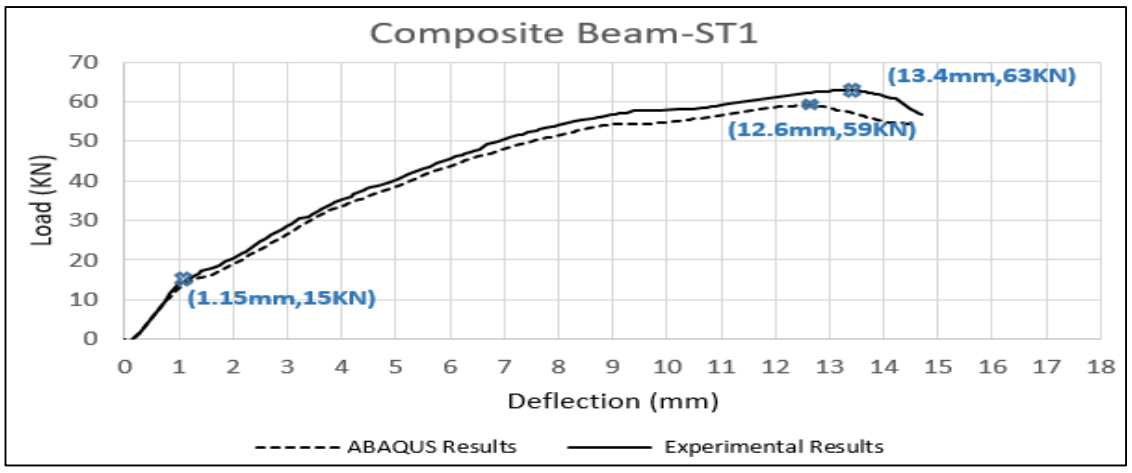

Fig. 5: Experimental and Numerical load-deflection Curves of ST1 Beam

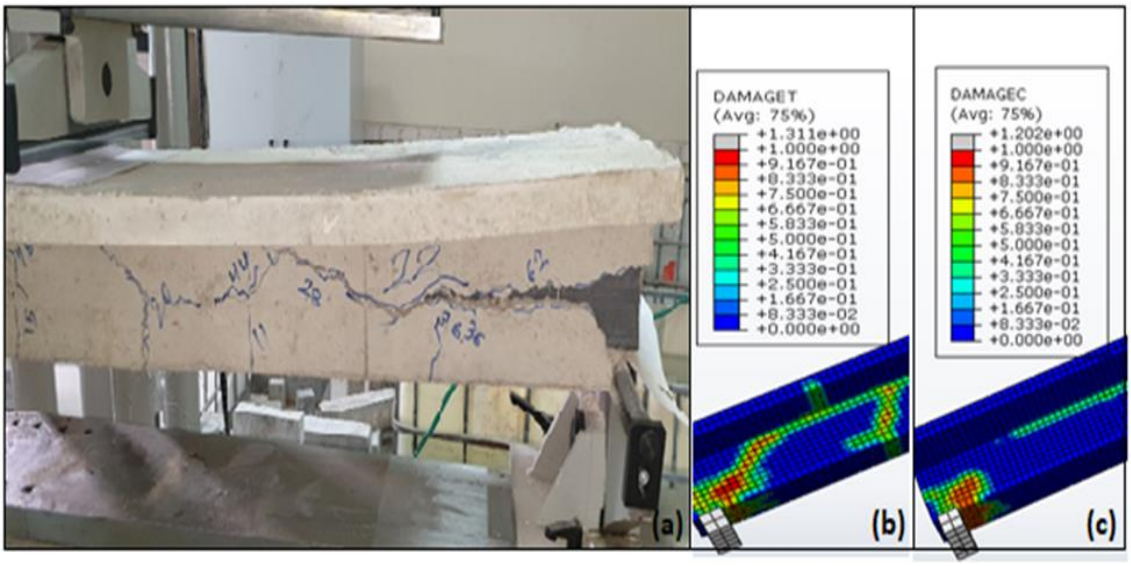

Fig.6: Validation of Experimental and Numerical Failure Modes of ST1 Beam

4.2 ST2 Specimen:

At initial stage of testing of ST2 beam, there was no inflection point in both fitted curves indicating full composite action. Then, by increasing the load, many tensile cracks have occurred leading to an acceptable variation of results with a difference in ultimate load and corresponding deflection of 3.9% and 0.69% respectively as displayed in Fig. 7.

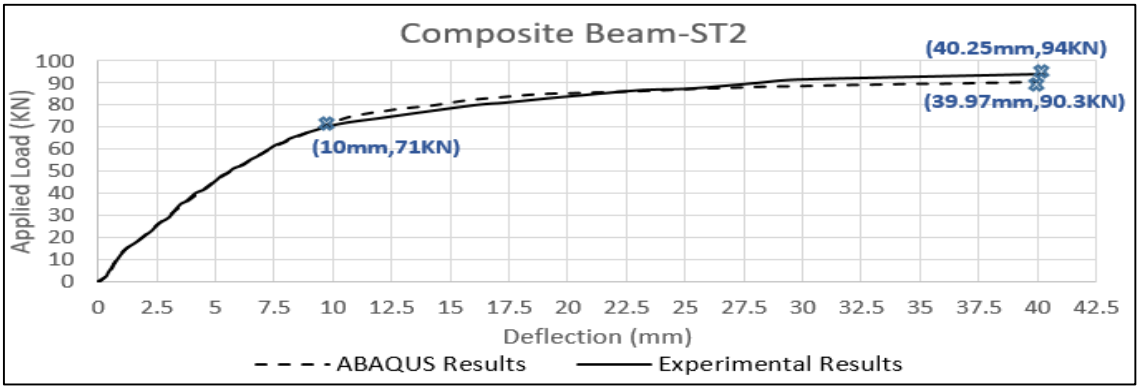

Fig. 7: Experimental and Numerical Load-Deflection Curves of ST2 Beam

Fig. 8 (a) and (b) also indicate satisfying simulation of numerical results showing a ductile behavior of the tested propagated across the deck thickness below the loading pads. In addition, small horizontal slippage was recorded during the experimental testing having a value of 0.5 cm at the bottom of the steel tube without any concrete spalling, as in Fig. 8 (c), and it was validated numerically in Fig.8(d) by horizontal displacement having a value between 3.6 and 7.19mm at the same mentioned location. Moreover, the absence of spalling at failure can be proved by the pattern of tensile crack propagation at supports showing the advantage of using steel mesh in providing good bonding and therefore better ductility.

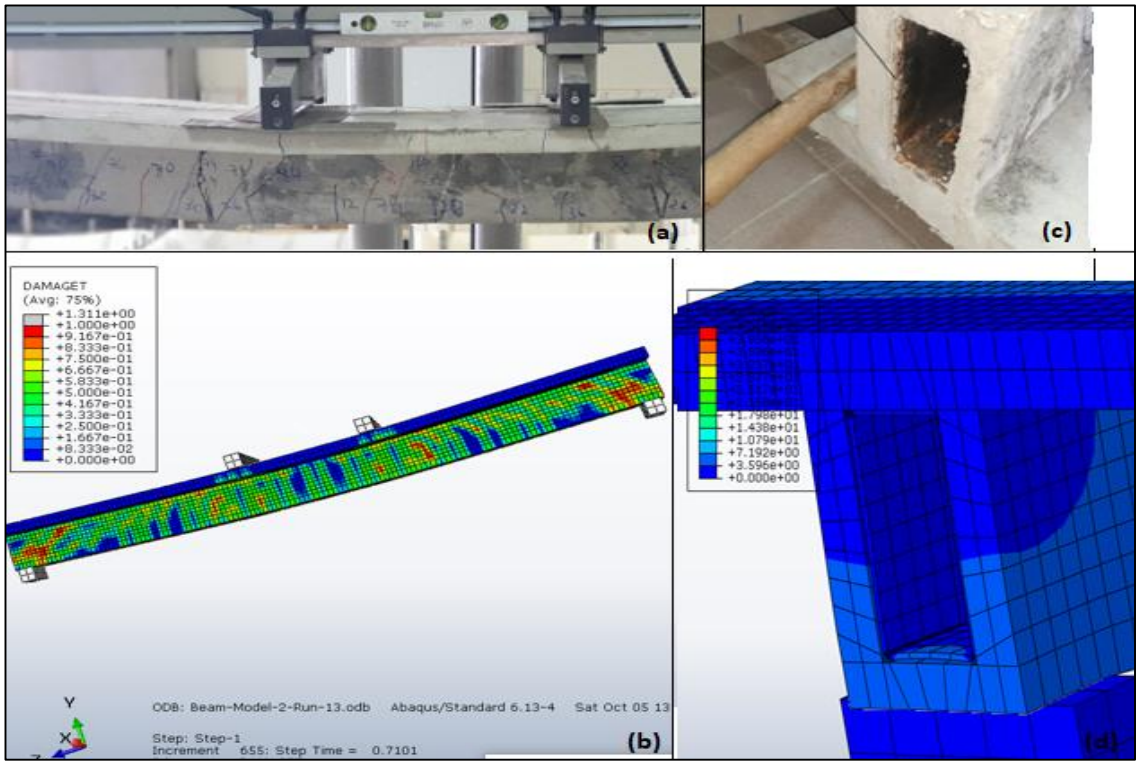

Fig.8: Validation of Experimental and Numerical Failure Modes of ST2 Beam

4.3 ST4 Specimen:

At the beginning of loading of ST4 beams in Fig. 9, there was full fitting between the two curves till reaching a load of approximately 30KN that can be explained by the formation of two flexural cracks at locations deprived from steel mesh causing reduction in material strength and stiffness. However, the later difference between experimental and numerical results is acceptable having a difference in ultimate capacities and corresponding deflection of 6.49% and 5.94% respectively.

In addition, Fig. 10 ensures exact numerical representation of the failure mode. For instant, the ABAQUS model showed generation of upward propagation of flexural tensile cracks at mid span with the obvious widening of two cracks generated initially (at 30KN load) at the sides of loading pads in the unmeshed zone. Also, the model displayed high compression damage below the deck indicating the propagation and widening of these two cracks below the deck as shown experimentally also. However, the compression damage at supports was seen in the form of fine cracks due to the presence of mesh providing good concrete bonding.

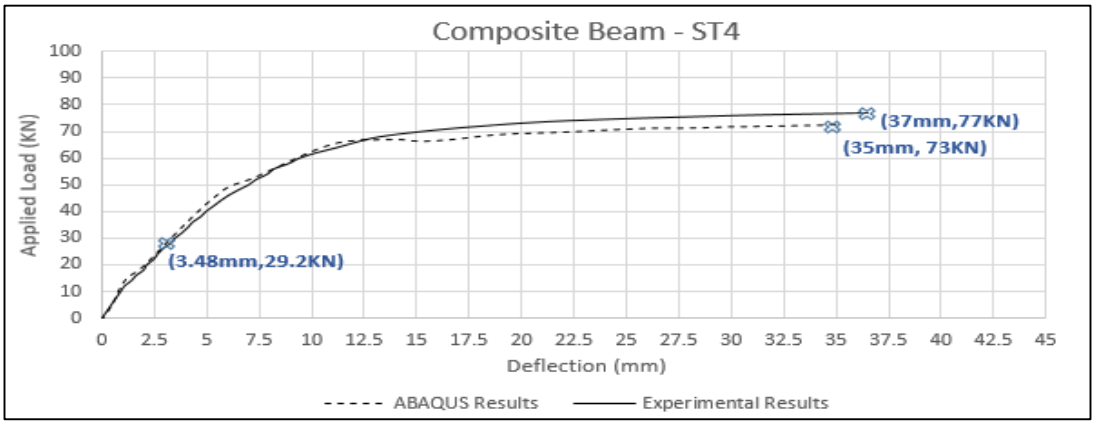

Fig.9: Experimental and Numerical Load-Deflection Curves of ST4 Beam

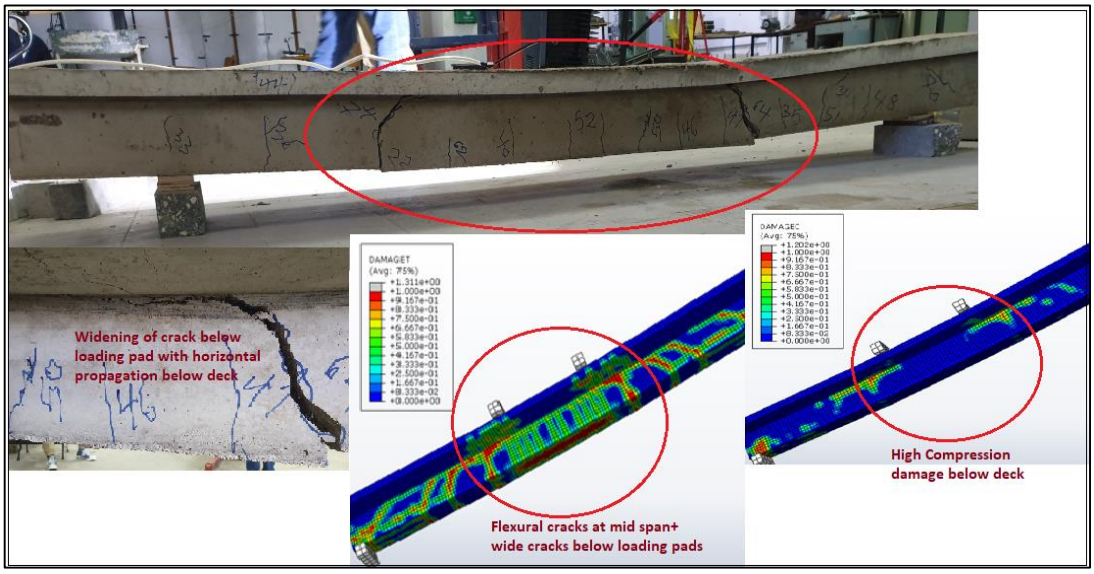

Fig. 10: Validation of Experimental and Numerical Failure Modes of ST4 Beam

4.4 SP1 Specimen:

As its seen in Fig.11, both curves increased linearly at early stages of loading till reaching a load of 13.7KN in experimental records and 14KN based on numerical results. After this load, a small neck occurred in both curves due to critical cracks formation resulting in drop of stiffness (slope) with small variation of results till reaching ultimate capacity. The difference of ultimate capacities and deflection between experimental and numerical simulations was 3.48% and 10.8% respectively.

Besides, from Fig.12, we can know that the failure mode of SP1 beam is characterized by the widening of two flexural cracks below the location of loading pads as well as beginning of enlargement of the horizontal cracks that were propagating towards the beam ends. The ABAQUS model has predicted the widening of two tensile flexural cracks as well as the propagation of horizontal cracks towards the beam ends and getting wider at ultimate capacity as displayed by the high horizontal compression damage. In addition, the presence of steel mesh provided good bonding at supports ending up in the formation of fine cracks without widening or spalling and prevented horizontal splitting and this was expected numerically by having stresses below the ultimate capacity of steel mesh. Furthermore, at ultimate capacity, propagation of fine cracks along the bottom of the deck was recorded both experimentally and numerically.

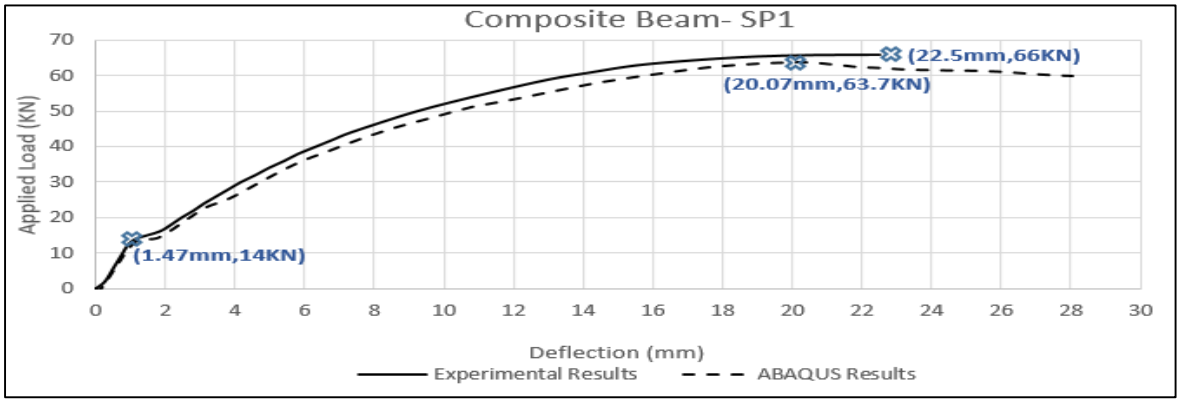

Fig. 11: Experimental and Numerical Load-Deflection Curves of SP1 Beam

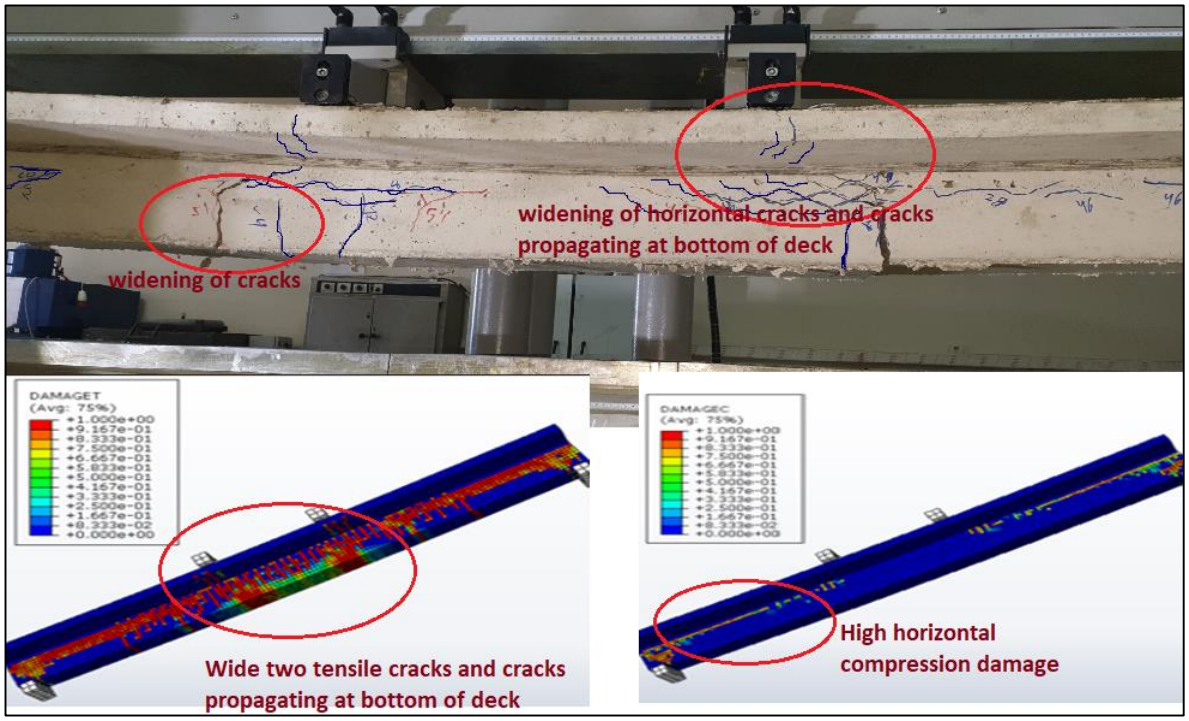

Fig.12: Validation of Experimental and Numerical Failure Modes of SP1 Beam

4.5 SP2 Specimen:

Both curves of Fig. 13 increase linearly till reaching a load of 10KN experimentally and 13.8KN numerically, at which a drop in the slope was recorded due to the formation of two main flexural cracks at the sides of loading pads. Then by increasing the load to a value of 34KN experimentally and 32KN numerically, another obvious drop in stiffness was detected till reaching the ultimate capacity. So, the numerical model has provided good fitting of the studied behavior with acceptable difference in the ultimate load capacity and corresponding deflection of 10.1% and 9.7% respectively.

Besides, Fig.14 shows good fitting of results regarding the expected failure mode. As we can see at early stages of loading, formation of two flexural cracks was detected at the location of loading pads in the unmeshed zone and then cracks were developed at new locations. After that, by increasing the applied load to 34KN, formation of horizontal cracks was seen at locations deprived from mesh. At ultimate capacity, widening of the two initial flexural cracks was seen along with the propagation of some cracks along the deck and this was expected numerically from the concrete tensile damage results. Furthermore, high horizontal compression damage was detected and can be explained by the large number of cracks propagating near the edges with widening of horizontal cracks in the unmeshed zone. However, at the edges of the beam, the presence of mesh prevented the widening of cracks at the location of supports subjected to high compression damage.

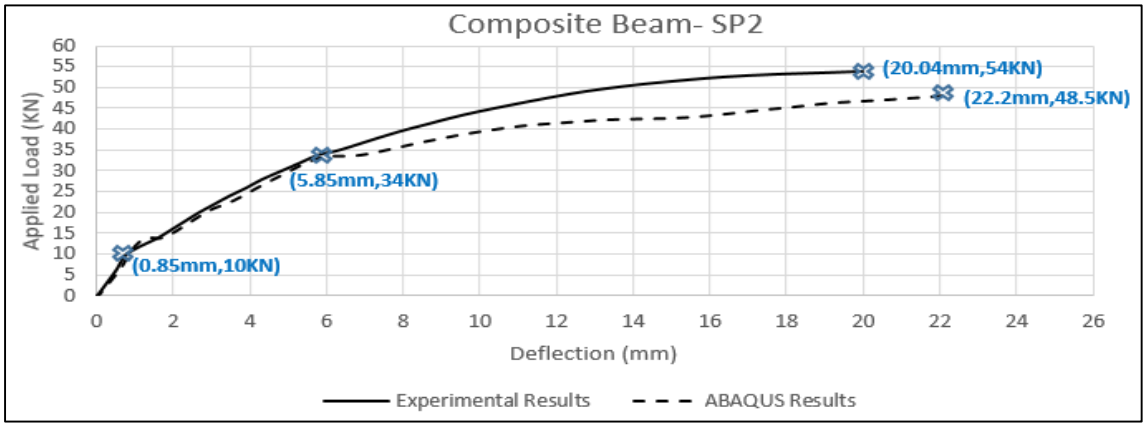

Fig.13: Experimental and Numerical Load-Deflection Curves of SP2 Beam

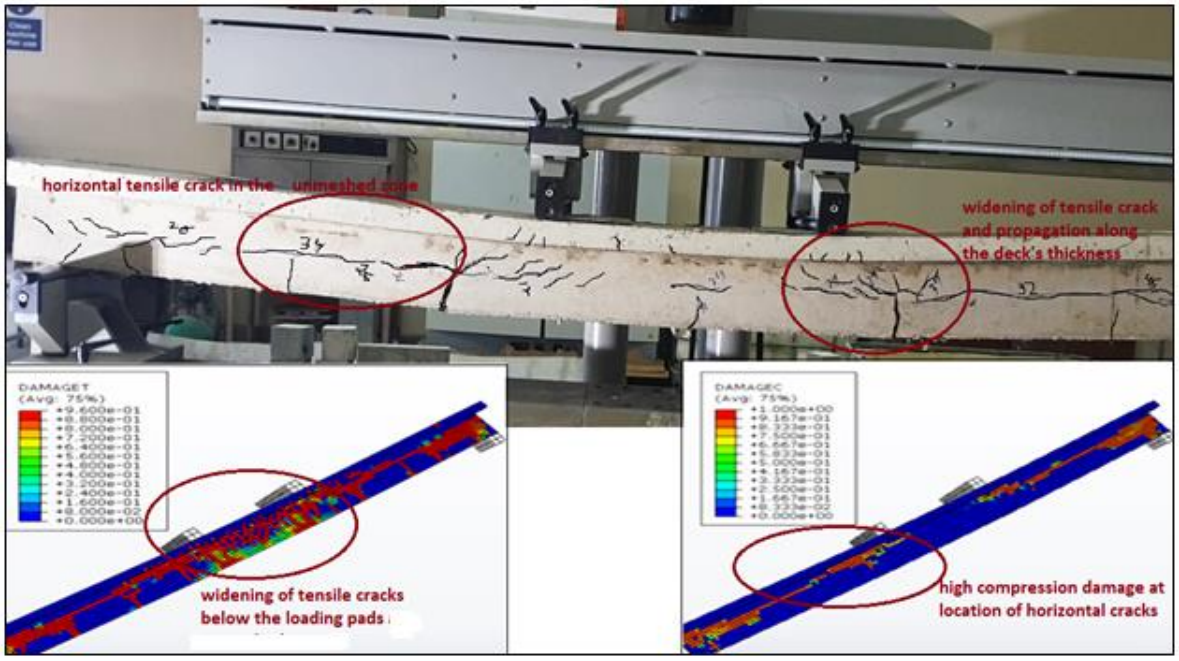

Fig.14: Validation of Experimental and Numerical Failure Modes of SP2 Beam

5. CONCLUSIONS

In this study, the flexural capacity and failure mode of innovative composite section was investigated experimentally and then verified numerically using ABAQUS finite element model. The importance of the studied composite section is related to its easy and fast fabrication as well as its ability of being part of precast long span floor system.

The following conclusions can be drawn from this investigation:

- The numerical model generated using ABAQUS software proved its ability in providing realistic simulation of the behavior of the studied composite beams having acceptable difference in ultimate capacities.
- Comparing the flexural capacities and ductility of ST beams, it's found that by increasing the percentage of steel mesh wrapping, the ultimate capacity and ductility are enhanced by 66.7% and 32.98% respectively for the case of full mesh wrapping relative to no mesh in ST beams.
- Both ST and SP beams that lack the presence of steel mesh wraps at the edges of the beam, have experienced the formation of wide horizontal cracks near the beam supports causing concrete splitting and spalling at the edges of the beam.
- Both ST and SP beams that are wrapped by 60% steel mesh, showed different pattern of cracks distribution along the beam length, but recorded similar failure modes of widening of two cracks initially formed at the sides of loading pads at the unmeshed zones without showing concrete splitting or spalling at highly compressive damaged locations.
- The large concrete cover at the bottom of SP specimens caused early formation and widening of flexural cracks at the bottom of the beam below the location of loading pads. This resulted in low ultimate capacity and ductility as expected from a circular steel pipe having same steel area.
- The 60% mesh wrapping specimen (ST4) can be considered as optimized section by providing ultimate capacity and good ductility which are close to the case of full mesh wrapping specimen.
- ST specimens experienced more favorable flexural behavior as compared to SP specimens of same percentage of mesh wrapping in terms of ultimate capacity and ductility.

REFERENCES

- Fan,H., Li,Q.S., Tuan,A.Y., Xu,L. Seismic analysis of the world's tallest building. Journal of Constructional Steel Research. 2009. 65(5). Pp. 1206-1215.DOI: 10.1016/j.jcsr.2008.10.005.
- Chan, S.L., Fong, M. Experimental and analytical investigations of steel and composite trusses.

Advanced Steel Construction. 2011. 7(1). Pp. 17-26. DOI: 10.18057/IJASC.2011.7.1.2.
- Kuhlmann,U., Breunig, S., Gölz, L., Pourostad, V., Stempniewski, L. New developments in steel and composite bridges. Journal of Constructional Steel Research.2020. DOI: 10.1016/j.jcsr.2020.106277.
- Kong, F., Huang, P., Han, B., Wang, X., Liua, C. Experimental study on behavior of corrugated steel-concrete composite bridge decks with MCL shape composite dowels. Engineering Structures.2021. DOI: 10.1016/j.engstruct.2020.111399
- Hu, Y., Zhao, J., Zhang, D., Li,Y. Cyclic performance of concrete-filled double-skin steel tube frames strengthened with beam-only-connected composite steel plate shear walls. Journal of Building Engineering.2020. DOI: 10.1016/j.jobe.2020.101376.
- Fujikura, S. and Bruneau, M. Dynamic analysis of multi hazard -resistant bridge piers having concrete filled steel tube under blast loading. Journal of Bridge Engineering.2012. 17(2). Pp.249-258. DOI:10.1061/(ASCE)BE.1943-5592.0000270.
- Fan, H., Li, Q.S., Tuan, A.Y., Xu, L. Seismic analysis of the world's tallest building. Journal of Constructional Steel Research. 2019. 65(5). Pp.1206-1215. DOI: 10.1016/j.jcsr.2008.10.005.
- Fu, Z., Wang, Q., Wang, Y., Ji,B. Bending Performance of lightweight Aggregate Concrete-Filled Steel Tube Composite Beam. KSCE Journal of Civil Engineering.2018. 22(10):3894-3902.
- Farhan, K., Shallal, M. EXPERIMENTAL BEHAVIOUR OF CONCRETE-FILLED STEEL TUBE COMPOSITE BEAMS. Archives of Civil Engineering. 2020. 64(2). Pp. 235-251. DOI: 10.24425/ace.2020.131807.
- Adithya, T., Monica Madhuri, N. Flexural behavior of concrete-filled steel tube beams. Anveshana's International Journal of Research in engineering and applied sciences.2017. 22(1). Pp. 2455-6300.
- Usach, C., Figueirido, D., Piquer, A. Effect of steel tube thickness on the behavior of CFST columns: Experimental tests and design assessment.2021.230(1). DOI: 10.1016/j.engstruct.2020.111687.
- **Zhou**, K., Hai Han, L. Experimental performance of concrete-encased CFST columns subjected to full-range fire including heating and cooling. Engineering Structures.2018. 165.Pp. 331-348.
- Wehbi,N., Masri, A. Fire resistance of built-up steel section completely encased in concrete. Journal of Engineering Science and Technology Review.2017.10(5). Pp.153-158.
- Hegyi, P., Dunai, L. Experimental study on ultra-lightweight-concrete encased cold-formed steel structures Part I: Stability behaviour of elements subjected to bending. Thin-Walled Structures. 2016. 101. Pp.75-84.
- El Basha, M., Hassan, K., Mohamed, M., Elnawawy, O. Efficiency of hollow reinforced concrete encased steel tube composite beams. International Journal of Civil Engineering and Technology (IJCIET).2018.9(3). Pp.720-735. ID: IJCIET_09_03_073.
- Weng, C.C, Yen, SI., Jiang, M.H. Experimental study on shear splitting failure of full –scale composite concrete encased steel beams. Journal of Structural Engineering.2002. 128(9).
- Tuma, N., Aziz, M. Flexural strength estimation for composite UHPC- tubular steel beam. Journal of Engineering Science and Technology.2020. 15(3). Pp. 1520-1541.
- Neelima, K., Shingade, V.S. Experimental study on performance of composite beams with and without shear reinforcement. International Journal of Engineering Research and Development.2016. 12(7). Pp. 10-16.
- Wehbi,N., Masri, A., Baalbaki,O. Experimental investigation on the flexural behavior of partially composite concrete-encased steel tubular beams. Magazine of Civil Engineering. Under review
- ABAQUS 13.1 Analysis User's Manual
- Lubliner, J., Oliver, J., Oller, S., Oñate, E. A Plastic-damage model for concrete. International Journal of Solids and Structures. 1989. 25. Pp. 299–329.
- J. Lubrliner. Plasticity Theory. Macmillan, New York (1990).
- Lee, J., Fenves, G. Plastic-damage model for cyclic loading of concrete structures. Journal of Engineering Mechanics.1998. 124(8). Pp. 892–900.